AIP Applied Physics Letters

Acoustic Bragg mirrors and cavities made using piezoelectric oxides

A. Soukiassian, W. Tian, D. A. Tenne, X. X. Xi, D. G. Schlom, N. D. Lanzillotti-Kimura, A. Bruchhausen, A. Fainstein, H. P. Sun, X. Q. Pan, A. Cros, and A. Cantarero

Citation: Applied Physics Letters **90**, 042909 (2007); doi: 10.1063/1.2432246
View online: http://dx.doi.org/10.1063/1.2432246
View Table of Contents: http://scitation.aip.org/content/aip/journal/apl/90/4?ver=pdfcov
Published by the AIP Publishing

Acoustic Bragg mirrors and cavities made using piezoelectric oxides

A. Soukiassian, W. Tian, D. A. Tenne,[a] X. X. Xi, and D. G. Schlom[b]
Materials Research Institute, The Pennsylvania State University, University Park, Pennsylvania 16802

N. D. Lanzillotti-Kimura, A. Bruchhausen, and A. Fainstein
Centro Atómico Bariloche and Instituto Balseiro, CNEA, 8400 San Carlos de Bariloche, Río Negro, Argentina

H. P. Sun and X. Q. Pan
Department of Materials Science and Engineering, University of Michigan, Ann Arbor, Michigan 48109

A. Cros and A. Cantarero
Materials Science Institute, University of Valencia, P.O. Box 22085, E-46071 Valencia, Spain

(Received 16 August 2006; accepted 13 December 2006; published online 24 January 2007)

The concept and design of acoustic Bragg mirrors and cavities made of multilayers of piezoelectric oxides with superior acoustic performance and potential applications in electronic and optical terahertz modulators are described. With these applications in mind the authors have grown phonon mirrors consisting of $BaTiO_3/SrTiO_3$ superlattices on $SrTiO_3$ substrates by reactive molecular-beam epitaxy and investigated their properties. Characterization of the superlattices by x-ray diffraction and high-resolution transmission electron microscopy reveals high structural quality with nearly atomically abrupt interfaces. The authors have observed folded acoustic phonons at the expected frequencies using uv Raman spectroscopy. © *2007 American Institute of Physics*.
[DOI: 10.1063/1.2432246]

Tailoring acoustic phonon properties is important for terahertz frequency phonon devices including the generation and amplification of coherent phonons.[1–6] Recently, terahertz acoustic cavities have been demonstrated with enormously amplified acoustic phonon-photon interaction,[2,7] leading to the possibility of modifying the lifetime of optical phonons through tailored anharmonic processes.[8] Acoustic cavities could also provide the required feedback mechanism of a phonon laser.[4,8] These and other important developments in terahertz acoustics are based mainly on compound semiconductors using mature epitaxial growth techniques such as molecular-beam epitaxy (MBE) that enable the construction of heterostructures with atomically flat interfaces by design.

Heterostructures of oxide materials such as $BaTiO_3$ and $SrTiO_3$, with strong coupling between sound, charge, and light, offer a nearly unexplored but rich terrain of versatile compounds with superior acoustic properties. They provide a range of acoustic impedances that can exceed the acoustic impedance mismatches in semiconductor heterostructures. In addition, they can be strongly piezoelectric, providing additional mechanisms that can significantly enhance sound-light coupling[9] and allowing electrical tuning of acoustic cavity wavelengths. Recently, room temperature ferroelectricity was observed in $SrTiO_3$ thin films under ~1% biaxial tensile strain.[10–12] Such strain could be attained at terahertz frequencies through coherent phonon generation using ultrafast laser excitation.[9] Because the light-sound interaction is greatly amplified in piezoelectric and ferroelectric materials,[13] including strain-enhanced heterostructures of ferroelectric $SrTiO_3$ and $BaTiO_3$,[12,14,15] these are very attractive for efficient phonon devices operating at terahertz frequencies.

In the present letter we propose acoustic Bragg mirrors and cavities made of $BaTiO_3/SrTiO_3$ heterostructures. Figure 1 shows their schematics, calculated acoustic reflectivity, and phonon field distribution.[16,17] The $BaTiO_3/SrTiO_3$ structures are compared with equivalent ones made of GaAs/AlAs, the materials system previously used for these acoustic structures,[2,7] and of $BaO/SrTiO_3$, another multilayer that can be grown by reactive MBE. A superlattice with a basic building block formed by two acoustic impedance-mismatched materials with respective layer thicknesses $\lambda/4$ and $3\lambda/4$ acts as an acoustic phonon Bragg mirror with stop band centered at $\omega = v/\lambda$. Here λ and v are the (material dependent) phonon wavelength and sound velocity, respectively.[2] The acoustic impedance mismatch $Z = (v_1\rho_1)/(v_2\rho_2) < 1$,[7] where v_j and ρ_j are the sound velocity and density of material j, respectively. For $BaTiO_3/SrTiO_3$ $Z = 0.75$, whereas $Z = 0.84$ for GaAs/AlAs and $Z = 0.66$ for $BaO/SrTiO_3$.[16] This difference in Z leads to enormous differences in device performance, as shown in Fig. 1. A (001)-oriented $BaTiO_3/SrTiO_3$ superlattice with a building block made of four unit cells of $SrTiO_3$ and eight unit cells of $BaTiO_3$ is close to having the ideal $(\lambda/4, 3\lambda/4)$ stacking. The mirror reflectivities R for superlattices with ten repeats are 0.878 for GaAs/AlAs, 0.987 for $BaTiO_3/SrTiO_3$, and 0.999 for $BaO/SrTiO_3$.[16] A $BaTiO_3/SrTiO_3$ phonon cavity may be constructed by enclosing a 21-unit-cell-thick (001) $BaTiO_3$ spacer, which is close to 2λ, between two $[(BaTiO_3)_8/(SrTiO_3)_4)]_{10}$ phonon mirrors, leading to a well centered cavity mode. Here the subscripts 4 and 8 indicate the thicknesses of the (001)-oriented $SrTiO_3$ and $BaTiO_3$ layers in unit cells and the subscript 10 indicates the number of times the $BaTiO_3/SrTiO_3$ bilayer is repeated.

As is evident from the plot in Fig. 1, a higher R results in a better cavity finesse. A consequence of the better finesse is a larger number of transit times of a phonon in the cavity before tunneling out through the mirrors. For the cavities

[a]Present address: Department of Physics, Boise State University, Boise, Idaho 83725.
[b]Electronic mail: schlom@ems.psu.edu

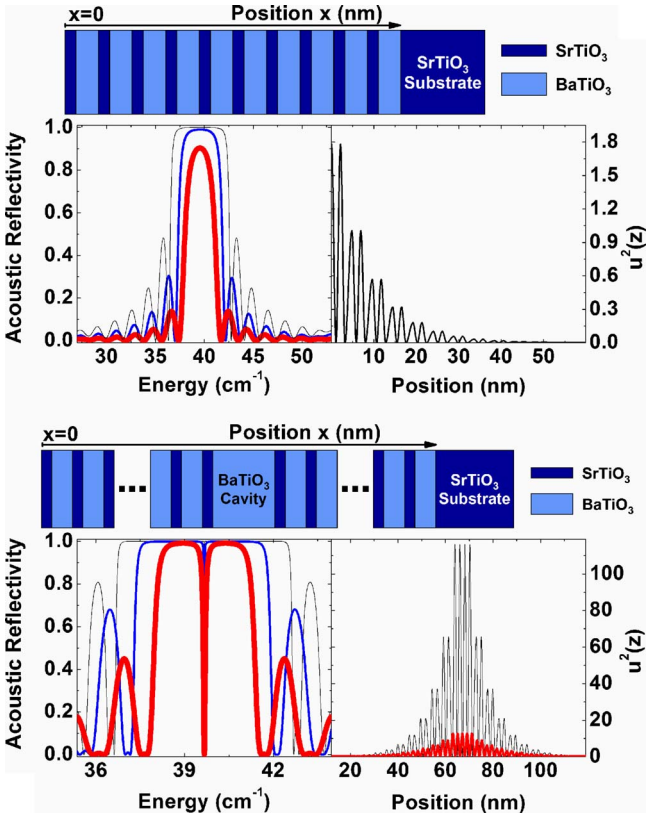

FIG. 1. (Color online) Top: Calculated acoustic reflectivity as a function of phonon energy (left) and square of phonon displacement along the growth axis z as a function of the distance into the mirror (right) for phonon mirrors consisting of a superlattice of (001)-oriented $BaTiO_3/SrTiO_3$ layers repeated ten times. Bottom: Calculated acoustic reflectivity as a function of phonon energy (left) and square of phonon displacement along the growth axis z as a function of the distance from the surface of the top mirror (right) for 2λ acoustic cavities enclosed by the superlattice phonon mirrors with ten repeats shown in the top panel. The increasing curve thicknesses correspond to $BaO/SrTiO_3$, $BaTiO_3/SrTiO_3$, and GaAs/AlAs, respectively. A schematic of the structure for the specific case of $BaTiO_3/SrTiO_3$ is shown.

shown, this corresponds to 8 for the GaAs/AlAs structure, 80 for $BaTiO_3/SrTiO_3$, and 1000 for $BaO/SrTiO_3$.[16] Concomitant with this increase in finesse, the square of the phonon displacement at the cavity center (indicative of the cavity Q factor and related to the acoustic energy deposited at the resonator) grows from ~12, to ~120, to ~1500 (given in relative units, for an incident phonon wave of amplitude equal to 1).[16] The latter, corresponding to $BaO/SrTiO_3$, is not shown in Fig. 1 for clarity.

The most important problem related to the growth of the heterostructures described above is the abruptness of the many ideally planar heterointerfaces on the atomic scale. Due to the extremely short phonon wavelength targeted for these structures ($\lambda \sim 5$ nm for the four-unit-cell thick $SrTiO_3$ and eight-unit-cell thick $BaTiO_3$ layers in the superlattice forming the phonon mirrors), the quality of the heterointerfaces plays a crucial role in the device performance. MBE has been used to create outstanding oxide superlattices with interface flatness and abruptness rivaling that of compound semiconductor superlattices grown by the same technique.[18]

Epitaxial $BaTiO_3/SrTiO_3$ superlattices were grown on TiO_2-terminated (001) $SrTiO_3$ substrates[19] by reactive MBE. The $BaTiO_3/SrTiO_3$ superlattices were grown by sequential deposition of the constituent monolayers at a background pressure of 5×10^{-7} Torr of molecular oxygen and a substrate temperature of 650–700 °C, as measured by an optical pyrometer. Additional details on the sample preparation are given elsewhere.[20]

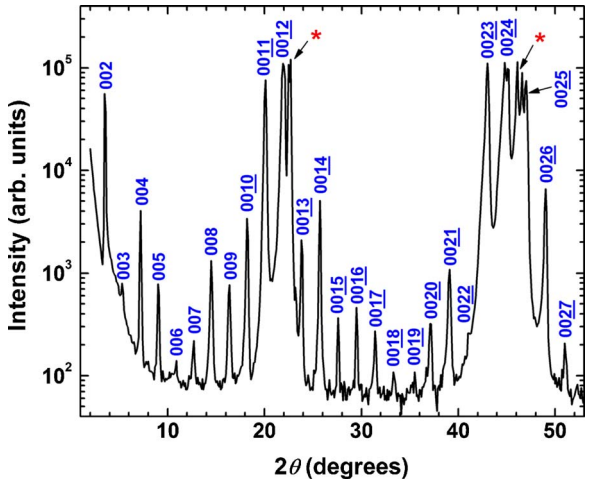

FIG. 2. (Color online) θ-2θ x-ray diffraction scan of a $[(BaTiO_3)_8/(SrTiO_3)_4]_{40}$ superlattice. Substrate peaks are marked by asterisks (*).

Four-circle x-ray diffraction with Cu $K\alpha$ radiation and high-resolution transmission electron microscopy (HRTEM) were used to structurally characterize the $[(BaTiO_3)_8/(SrTiO_3)_4]_{40}$ superlattice. A θ-2θ x-ray diffraction scan is shown in Fig. 2(a). Nearly all superlattice peaks are present for $2\theta < 55°$, which is an indication of atomically sharp interfaces between $BaTiO_3$ and $SrTiO_3$ layers. The superlattice period, $d_{SL}=48.25\pm0.01$ Å, was obtained from a Nelson-Riley analysis[21] of these peaks. The in-plane orientation relationship between the $[(BaTiO_3)_8/(SrTiO_3)_4]_{40}$ superlattice and the (001) $SrTiO_3$ substrate was determined by a ϕ scan of the $10\underline{12}$ superlattice peak. The result is that the [100] superlattice direction is aligned parallel to the [100] $SrTiO_3$ substrate direction.[20] From the position of the $10\underline{12}$ superlattice peak and the out-of-plain lattice parameter, the in-plane lattice parameter $a=3.946\pm0.003$ Å was determined. This in-plane lattice constant lies between that of $SrTiO_3$ and $BaTiO_3$, as expected for a partially relaxed $[(BaTiO_3)_8/(SrTiO_3)_4]_{40}$ superlattice that is no longer commensurately strained to the underlying (001) $SrTiO_3$ substrate. An analogous phonon mirror with fewer repeats, i.e., $[(BaTiO_3)_8/(SrTiO_3)_4]_{10}$, was fully commensurate with the underlying (001) $SrTiO_3$ substrate.[22] The full width at half maximum of the rocking curve of the $00\underline{23}$ peak of the $[(BaTiO_3)_8/(SrTiO_3)_4]_{40}$ superlattice was 0.06°. A cross-sectional HRTEM image of the same superlattice is shown in Fig. 3. It reveals that the superlattice has nearly atomically abrupt interfaces. The interface roughness determined between the $BaTiO_3$ and $SrTiO_3$ layers is within one unit cell.

Raman scattering is a powerful technique to monitor the phonon properties of acoustic devices.[2,7,8] The challenge with oxide heterostructures lies in the large optical gaps, implying that Raman experiments with visible lasers are hindered by the small photoelastic constants, and the overwhelming contribution of the $SrTiO_3$ substrate. It has recently been shown that uv Raman spectroscopy can be used for ferroelectric thin films and superlattices.[22] We used a uv-optimized Jobin-Yvon T64000 triple spectrometer with a N_2-cooled multichannel coupled-charge-device detector

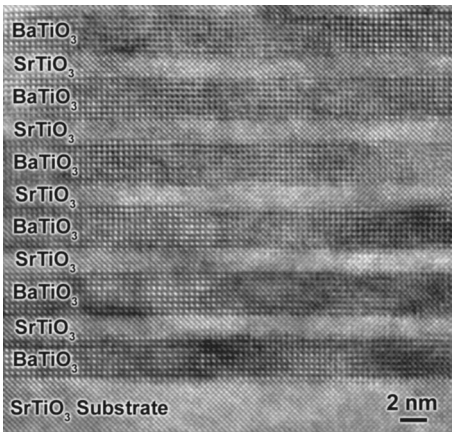

FIG. 3. Cross-sectional HRTEM image of a $[(BaTiO_3)_8/(SrTiO_3)_4]_{40}$ superlattice grown on a (001) $SrTiO_3$ substrate.

and the $\lambda=351.1$ nm line of an Ar laser for excitation. A measured room temperature Raman spectrum for the same $[(BaTiO_3)_8/(SrTiO_3)_4]_{40}$ superlattice in the low frequency region, obtained with polarizations parallel to [100] in backscattering along the growth c axis, is shown in Fig. 4. A clear doublet due to the folded longitudinal acoustic (LA) phonon modes is observed. The expected energy of the LA doublet can be derived by evaluating the acoustic modes of the superlattice with a Rytov continuum model[23] and using the wave vector transferred in the Raman scattering process, $q=4\pi n/\lambda$. To evaluate the latter, shown with the horizontal dashed line in the top panel of Fig. 4, the index of refraction of the superlattice at 351.1 nm ($n=2.88$) was measured using variable-angle ellipsometry. The folded phonon dispersion, calculated using the c-axis phonon velocities $v_{SrTiO_3}=7848.5$ m/s and $v_{BaTiO_3}=5420$ m/s, is displayed in the top panel of Fig. 4.[24,25] The predicted Raman doublet energies, corresponding to the intersection between the phonon dispersion and the transferred wave vector q, match precisely the experimental peaks. We also show in Fig. 4 the Raman spectrum obtained with a photoelastic model for the Raman efficiency.[23] The calculated curve was Gaussian convoluted to account for the spectrometer resolution ($2\sigma=3$ cm^{-1}). The agreement between the measured and calculated spectra is extremely good, both for the position and the relative intensity of the peaks.

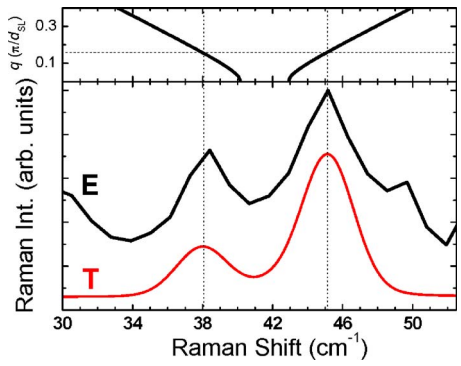

FIG. 4. (Color online) Bottom: Folded acoustic phonon modes measured by uv Raman scattering (E) in comparison with a photoelastic model calculation of the Raman efficiency (T). Top: Folded acoustic phonon dispersion obtained with a continuum Rytov model. The horizontal dashed line indicates the wave vector q transferred in the Raman scattering process.

In conclusion, we propose terahertz acoustic mirrors and cavities based on multilayers of $BaTiO_3$, $SrTiO_3$, and BaO. These structures exploit the acoustic and ferroelectric properties of oxides for superior performance. Our results demonstrate the feasibility to design, fabricate, and characterize oxide piezoelectric acoustic devices.

This work is partially supported by ONR under Grant Nos. N00014-03-1-0721 (A.S., W.T., and D.G.S.) and N00014-04-1-0426 (A.S., W.T., and D.G.S.) monitored by Dr. Colin Wood, by NSF under Grant No. DMR-0507146 (A.S., D.G.S., H.P.S., X.Q.P., and X.X.X.), and by DOE under Grant No. DE-FG02-01ER45907 (D.A.T. and X.X.X.). One of the authors (A.F.) acknowledges support from ONR (U.S.) and CONICET (Argentina).

[1] N. M. Stanton, R. N. Kini, A. J. Kent, M. Henini, and D. Lehmann, Phys. Rev. B **68**, 113302 (2003).
[2] M. Trigo, A. Bruchhausen, A. Fainstein, B. Jusserand, and V. Thierry-Mieg, Phys. Rev. Lett. **89**, 227402 (2002).
[3] A. Bartels, T. Dekorsy, H. Kurz, and K. Köhler, Phys. Rev. Lett. **82**, 1044 (1999).
[4] P. A. Fokker, J. I. Dijkhuis, and H. W. de Wijn, Phys. Rev. B **55**, 2925 (1997).
[5] I. Camps, S. S. Makler, H. M. Pastawski, and L. E. F. Foa Torres, Phys. Rev. B **64**, 125311 (2001).
[6] J. Chen, J. B. Khurgin, and R. Merlin, Appl. Phys. Lett. **80**, 2901 (2002).
[7] P. Lacharmoise, A. Fainstein, B. Jusserand, and V. Thierry-Mieg, Appl. Phys. Lett. **84**, 3274 (2004).
[8] M. F. Pascual Winter, A. Fainstein, M. Trigo, T. Eckhause, R. Merlin, A. Cho, and J. Chen, Phys. Rev. B **71**, 085305 (2005).
[9] C.-K. Sun, J.-C. Liang, and X.-Y. Yu, Phys. Rev. Lett. **84**, 179 (2000).
[10] Y. L. Li, S. Choudhury, J. H. Haeni, M. D. Biegalski, A. Vasudevarao, A. Sharan, H. Z. Ma, J. Levy, V. Gopalan, S. Trolier-McKinstry, D. G. Schlom, Q. X. Jia, and L. Q. Chen, Phys. Rev. B **73**, 184112 (2006).
[11] M. D. Biegalski, Y. Jia, D. G. Schlom, S. Trolier-McKinstry, S. K. Streiffer, V. Sherman, R. Uecker, and P. Reiche, Appl. Phys. Lett. **88**, 192907 (2006).
[12] J. H. Haeni, P. Irvin, W. Chang, R. Uecker, P. Reiche, Y. L. Li, S. Choudhury, W. Tian, M. E. Hawley, B. Craigo, A. K. Tagantsev, X. Q. Pan, S. K. Streiffer, L. Q. Chen, S. W. Kirchoefer, J. Levy, and D. G. Schlom, Nature (London) **430**, 758 (2004).
[13] P. A. Fleury and P. D. Lazay, Phys. Rev. Lett. **26**, 1331 (1971).
[14] J. B. Neaton and K. M. Rabe, Appl. Phys. Lett. **82**, 1586 (2003).
[15] K. J. Choi, M. Biegalski, Y. L. Li, A. Sharan, J. Schubert, R. Uecker, P. Reiche, Y. B. Chen, X. Q. Pan, V. Gopalan, L.-Q. Chen, D. G. Schlom, and C. B. Eom, Science **306**, 1005 (2004).
[16] These values are calculated using the bulk (unstrained) properties of these materials.
[17] S. Mizuno and S. I. Tamura, Phys. Rev. B **45**, 734 (1992).
[18] D. G. Schlom, J. H. Haeni, J. Lettieri, C. D. Theis, W. Tian, J. C. Jiang, and X. Q. Pan, Mater. Sci. Eng., B **87**, 282 (2001).
[19] G. Koster, B. L. Kropman, G. J. H. M. Rijnders, and D. H. A. Blank, Appl. Phys. Lett. **73**, 2920 (1998).
[20] A. Soukiassian, W. Tian, V. Vaithyanathan, H. P. Sun, X. Q. Pan, Y. L. Li, L. Q. Chen, Q. X. Jia, K. J. Choi, D. M. Kim, C. B. Eom, A. Bruchhausen, N. D. Lanzillotti-Kimura, A. Fainstein, R. S. Katiyar, A. Cantarero, D. A. Tenne, X. X. Xi, and D. G. Schlom (unpublished).
[21] J. B. Nelson and D. P. Riley, Proc. Phys. Soc. London **57**, 160 (1945).
[22] D. A. Tenne, A. Bruchhausen, N. D. Lanzillotti-Kimura, A. Fainstein, R. S. Katiyar, A. Cantarero, A. Soukiassian, V. Vaithyanathan, J. H. Haeni, W. Tian, D. G. Schlom, K. J. Choi, D. M. Kim, C. B. Eom, H. P. Sun, X. Q. Pan, Y. L. Li, L. Q. Chen, Q. X. Jia, S. M. Nakhmanson, K. M. Rabe, and X. X. Xi, Science **313**, 1614 (2006).
[23] B. Jusserand and M. Cardona, in *Light Scattering in Solids V*, edited by M. Cardona and G. Güntherodt (Springer, Heidelberg, 1989), Vol. 66, pp. 49–146.
[24] J. B. Wachtman, Jr., M. L. Wheat, and S. Marzullo, J. Res. Natl. Bur. Stand., Sect. A **67**, 193 (1963).
[25] M. Zgonik, P. Bernasconi, M. Duelli, R. Schlesser, P. Gunter, M. H. Garrett, D. Rytz, Y. Zhu, and X. Wu, Phys. Rev. B **50**, 5941 (1994).